Electronic Supplementary Information (ESI)

Unusual oxidase-mimetic catalytic performance surpassing peroxidase in amorphous CoO_x: Underlying mechanism and toward a novel H_2O_2-related detection paradigm

Zhijian Bu[1, #], Jinjin Liu[1, #, *], Zheng Tang[1, 2], Hao Liang[1], Qinqin Bai[1], Shuangquan Liu[2], Xiangheng Niu[1, 2, *]

[1] School of Public Health, Hengyang Medical School, University of South China, Hengyang 421001, P. R. China

[2] The First Affiliated Hospital, Hengyang Medical School, University of South China, Hengyang 421001, P. R. China

[#] Authors who contributed to the work equally

[*] To whom correspondence should be addressed. E-mail: 2022000136@usc.edu.cn (J. Liu); niuxiangheng@usc.edu.cn (X. Niu)

1. Experimental details

1.1. Reagents and instruments

Cobalt(II) chloride hexahydrate ($CoCl_2 \cdot 6H_2O$), fructose, lactose, sucrose, maltose, ascorbic acid (AA), thiourea, and glucose oxidase (GOx) were obtained from Shanghai Aladdin Biochemical Technology Co., Ltd. (Shanghai, China). Hydrogen peroxide (H_2O_2) was purchased from Shanghai Titan Scientific Co., Ltd. (Shanghai, China). 3,3′,5,5′-Tetramethylbenzidine (TMB) and acetic acid (HAc) were purchased from Shanghai Macklin Biochemical Technology Co., Ltd. (Shanghai, China). Sodium acetate (NaAc) was purchased from Sinopharm Chemical Reagent Co., Ltd. (Shanghai, China). All the reagents were dissolved in deionized water.

The X-ray diffraction (XRD) characterization of samples was obtained from a Rigaku SmartLab SE instrument. Scanning electron microscopy (SEM) was carried out on a ZEISS Sigma 300 instrument. X-ray photoelectron spectroscopy (XPS) was conducted on a Thermo Scientific Nexsa instrument. The transmission electron microscopy (TEM) images of materials were obtained from a JEOL JEM F200 apparatus. The elemental component of materials was examined by inductively coupled plasma atomic emission spectrometry (ICP-AES) on an Agilent 720 instrument. Electron paramagnetic resonance (EPR) measurements were carried out on a Bruker EMXplus instrument. Ultraviolet-visible (UV-vis) absorption spectroscopy was performed on a Shimadzu 2600i spectrophotometer.

1.2. Synthesis of amorphous CoO_x

$CoCl_2 \cdot 6H_2O$ (120 mg) was dispersed in 20 mL deionized water and transferred into

a 50 mL flask. Subsequently, $NaBH_4$ aqueous solution (40 mg/mL, 4 mL) was added dropwise. Upon the contact of the two solutions, the solution color darkened rapidly, and some black solids were produced with the formation of a large number of bubbles. The resulting black suspension was continuously stirred at 30°C for 24 hours. Following this, the obtained tawny suspension was subjected to centrifugation and washed with deionized water several times. Finally, the amorphous CoO_x powder was collected by freeze drying for subsequent use.

For the treatment of CoO_x by H_2O_2, CoO_x (75 mg) was first dissolved in 15 mL of acetate buffer solution (0.2 M, pH 4.0), and subsequently 5 mL of H_2O_2 (9.8 M) was added to the solution to reach a final concentration of 2.45 M. The mixture was then transferred into a 50 mL beaker and stirred continuously for 1 h. Finally, the product was washed three times with deionized water and subjected to freeze-drying.

1.3. Oxidase-like activity of amorphous CoO_x

The oxidase-like activity of amorphous CoO_x was verified by the catalytic oxidation of TMB. First, 800 μL acetate buffer (0.2 mM, pH 4.0), 100 μL CoO_x solution (0.25 mg/mL), and 100 μL TMB solution (5 mM) were mixed in a 1.5 mL centrifuge tube, keeping the total volume of the mixed solution at 1 mL. Then, UV-vis absorption spectra of the reaction system were examined after incubation at room temperature for 10 minutes.

After optimizing the catalytic reaction conditions of amorphous CoO_x, its oxidase-like activity was evaluated by steady-state kinetic analysis. In detail, 800 μL acetate buffer (0.2 mM, pH 4.0) and 100 μL CoO_x solution (0.25 mg/mL) were first mixed, and

then different concentrations of TMB solution (100 μL) were added. The reaction system was measured by UV-vis at the wavelength of 652 nm within 180 seconds. During measurements, the reaction rate was calculated based on the Lambert-Beer law, and the molar extinction coefficient of oxTMB at 652 nm was 39000 M^{-1} cm^{-1}. Thus, the enzymatic kinetic curve of TMB was obtained. The kinetic parameters were obtained using the Lineweaver-Burk double-reciprocal plot: $1/V = K_m/(V_{max}[S]) + 1/V_{max}$, where V was the reaction velocity, V_{max} was the maximal reaction velocity, [S] was the substrate concentration, and K_m was the Michaelis-Menten constant.

1.4. Influence of H_2O_2 on the catalytic performance of amorphous CoO_x

The obtained amorphous CoO_x had double enzyme-like activities. By using CoO_x+TMB as the oxidase-like activity group and CoO_x+TMB+H_2O_2 as the peroxidase-like activity group, the two groups were first incubated at room temperature for 10 minutes, and then their absorbances were determined by UV-vis. The two catalytic activities could be assessed by comparing the absorbances of the two groups under identical conditions. When changing the concentration of H_2O_2 added to the CoO_x+TMB reaction system and measuring the absorbance change, the effect of H_2O_2 on amorphous CoO_x catalytic performance was explored.

1.5. Turn-off colorimetric detection of glucose

Glucose could be oxidized to produce H_2O_2 under the action of GOx, which further affected the catalytic performance of amorphous CoO_x, and thus quantitative detection of glucose could be achieved. In detail, 600 μL acetate buffer (0.2 mM, pH 4.0), 100 μL CoO_x solution (0.25 mg/mL), 100 μL GOx (1 mg/mL), and different concentrations

of glucose solution (100 μL) were mixed and incubated at 37℃ for 10 minutes. Then, 100 μL TMB solution (5 mM) was added to start color development, and the system absorbance was measured by UV-vis after reaction for 10 minutes at room temperature.

For real sample analysis, the serum samples received from hospital were diluted 100 times to obtain the final test samples. 100 μL diluted serum was added into a mixture containing 600 μL acetate buffer (0.2 mM, pH 4.0), 100 μL CoO_x solution (0.25 mg/mL) and 100 μL GOx solution (5 mg/mL). After incubating at 37℃ for 10 minutes, 100 μL TMB solution (5 mM) was added for reaction for another 10 minutes, and the UV-vis absorption spectra were measured by UV-vis.

2. Supplementary figures and tables

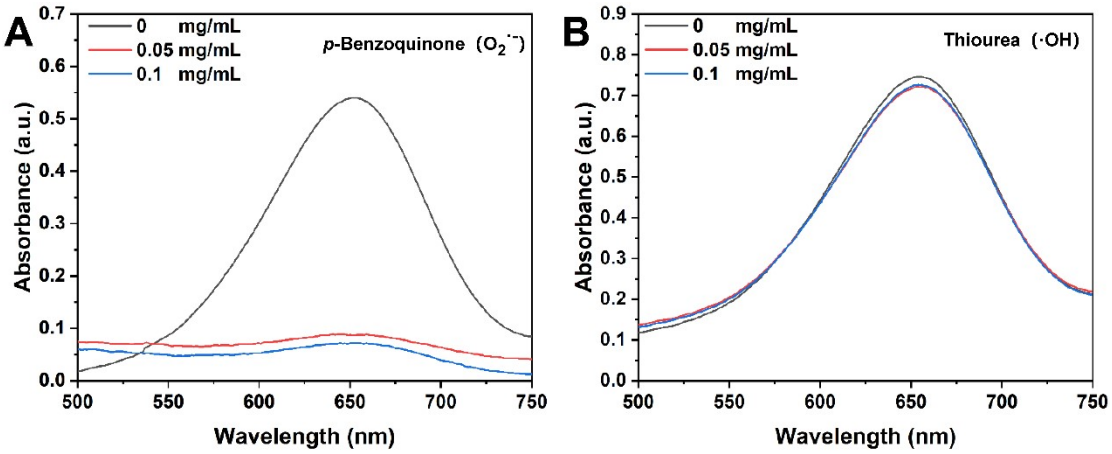

Figure S1. UV-vis absorption spectra of the CoO_x+TMB system in the presence of *p*-benzoquinone (A) or thiourea (B).

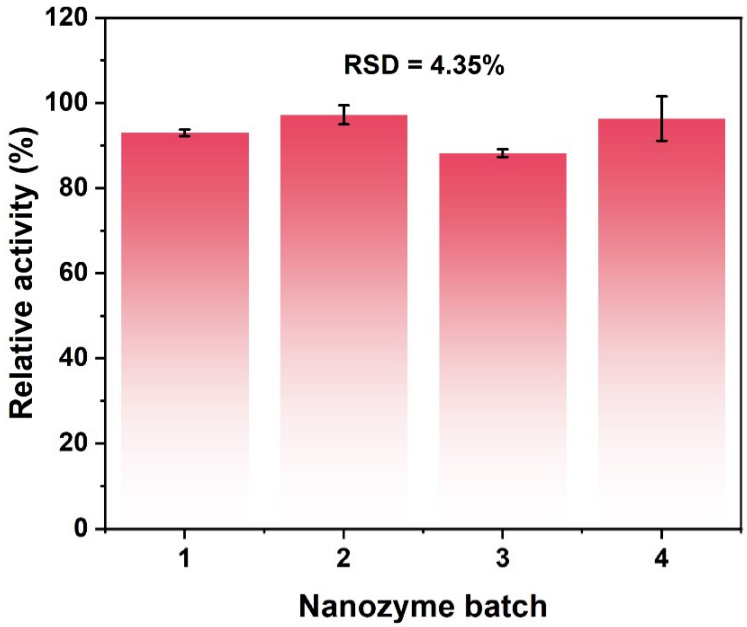

Figure S2. Batch stability of the oxidase-like activity of amorphous CoO_x.

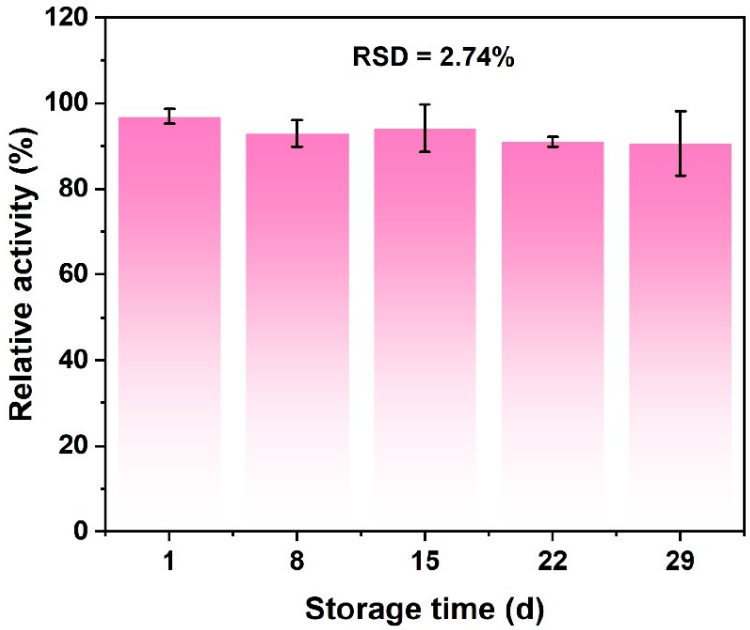

Figure S3. Storage stability of the oxidase-like activity of amorphous CoO_x.

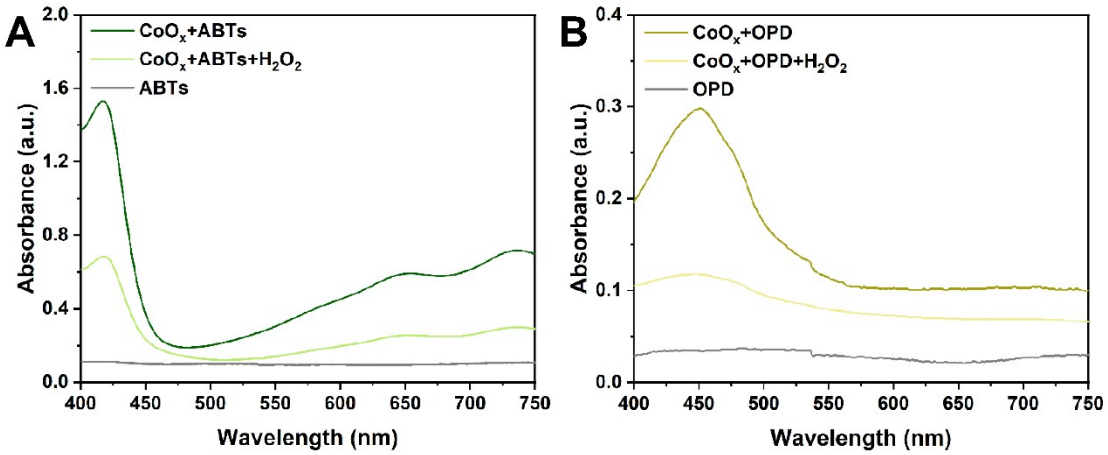

Figure S4. Catalytic response of amorphous CoO_x toward ABTS (A) and OPD (B) with or without H_2O_2.

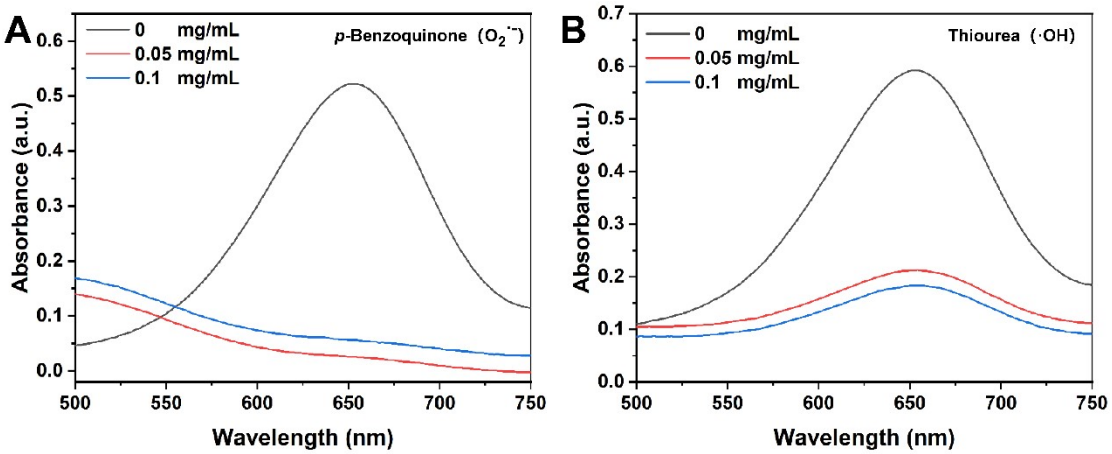

Figure S5. UV-vis absorption spectra of the CoO_x+TMB+H_2O_2 system in the presence of *p*-benzoquinone (A) or thiourea (B).

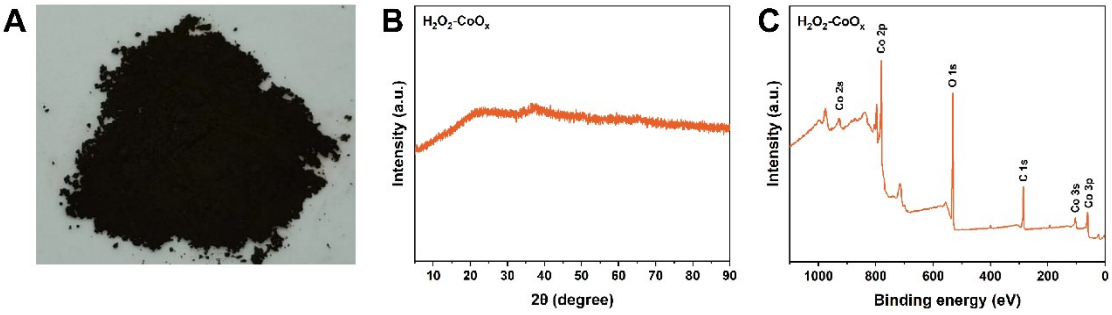

Figure S6. (A) Photograph, (B) XRD pattern, and (C) survey XPS pattern of the CoO_x material treated by H_2O_2.

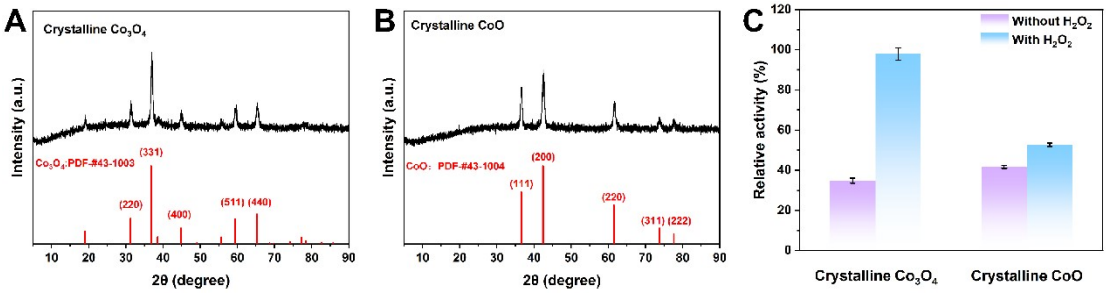

Figure S7. (A) XRD pattern of the Co_3O_4 material synthesized. (B) XRD pattern of the CoO material synthesized. (C) Comparison of oxidase- and peroxidase-like activities of crystalline Co_3O_4 and CoO.

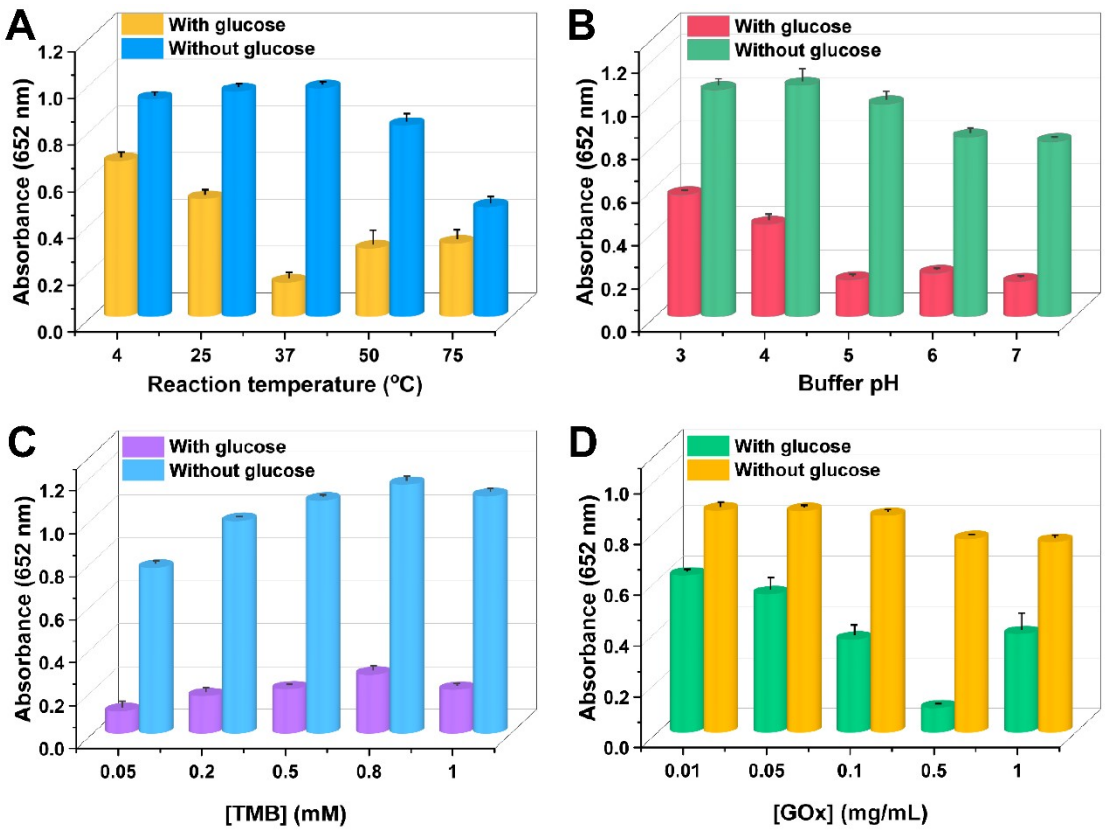

Figure S8. Effects of reaction temperature (A), buffer pH (B), TMB concentration (C), and GOx concentration (D) on the GOx+CoO_x+TMB system with or without the presence of glucose.

Table S1. Comparison of kinetic parameters of different nanozymes.

Nanozyme	**Substrate**	K_m **(mM)**	V_{max} **(10^{-8}, M/s)**	**Ref.**
Mn_3O_4	TMB	0.1896	28	[1]
SA-FeNC	TMB	0.836	10.57	[2]
Nanoceria	TMB	0.42	10.04	[3]
PPy@CuNi-ZIF-67	TMB	0.025	4.76	[4]
CeO_2 NPs	TMB	0.212	2.594	[5]
CoO_x	TMB	0.017	6.22	Our work

Table S2. Comparison of the binding energy peak positions of Co $2p_{1/2}$ and Co $2p_{3/2}$ in the CoO_x and H_2O_2-CoO_x samples determined by XPS.

Material	**Co $2p_{1/2}$ (eV)**	**Co $2p_{3/2}$ (eV)**
CoO_x	796.88	781.28
H_2O_2-CoO_x	795.86	780.58

Table S3. Comparison of the ratio of Co^{3+} to Co^{2+} in the CoO_x and H_2O_2-CoO_x samples determined by XPS.

Material	**Co^{3+}**	**Co^{2+}**	**Co^{3+}/Co^{2+}**
CoO_x	68.1%	31.9%	2.13
H_2O_2-CoO_x	46.6%	53.4%	0.87

Table S4. Relative proportions of O_A, O_V, and O_L in the CoO_x and H_2O_2-CoO_x samples determined by XPS.

Material	**O_A**	**O_V**	**O_L**
CoO_x	40.9%	38.3%	20.8%
H_2O_2-CoO_x	11.2%	49.1%	39.7%

Table S5. Detection performance comparison of our colorimetric method with previous ones for glucose detection.

Material	Sensing type	Detection range	LOD	Ref.
Fe-MIL-88B-NH_2	Turn-on	1~500 μM	0.487 μM	[6]
FeN/GQDs	Turn-on	1~300 μM	0.36 μM	[7]
Hemin-CDs	Turn-on	2.5~300 μM	1.026 μM	[8]
Pt-ONDs/AuBPs	Turn-on	0.2~400 μM	0.2 μM	[9]
$ZnIrO_x$/ZnIrMOFs	Turn-on	2.66~319 μM	1.9 μM	[10]
CoO_x	Turn-off	2~800 μM	0.09 μM	Our work

Table S6. Detection results of our method for glucose in real serum samples.

Sample	Detected (mM, n=3)*	Clinical result (mM)	Relative error (%)
#1	6.2±0.3	6.0	3.3
#2	7.1±0.4	7.5	-5.3
#3	6.8±0.5	6.5	4.6
#4	5.1±0.3	5.6	-8.9
#5	8.3±0.3	8.4	-1.2

* The samples were diluted 100 times and then tested. The detection results reported here had been converted into original levels in the serum samples obtained from hospital.

3. References

[1] J. Liang, D. Duan, L. Sun, J. Li, M. Wang, Z. Chang, R.F. Thorne, C. Chen, D. Duan, High-sensitivity colorimetric sensor based on oxidase-like Mn_3O_4 nanozyme for Cys detection, Sensors and Actuators Reports, 9 (2025) 100296.

[2] F. Liu, F. Jiao, T. Wang, Z. Li, H. Song, S. Wu, X. Zhang, H. Wang, C. Chen, Y. Lu, Free reactive oxygen species-independent dual enzymatic activity of iron single-atom catalyst for hydrogel-assisted portable visual analysis, Journal of Colloid and Interface Science, 686 (2025) 420-429.

[3] H. Cheng, S. Lin, F. Muhammad, Y.W. Lin, H. Wei, Rationally modulate the oxidase-like activity of nanoceria for self-regulated bioassays, ACS Sensors, 1 (2016) 1336-1343.

[4] L. Nie, J. Xia, J. Liao, N. Liu, M. Xu, D. Meng, W. Liu, Q. Zhou, C. Chen, Rapid visual detection of glutathione in vegetables and distinguishing multiple sulfur-containing compounds by smartphone-assisted sensor based on calcined PPy@CuNi-ZIF-67 nanozyme with enhanced oxidase-like activity, Food Chemistry, 474 (2025) 143189.

[5] N. Zhang, Y. Du, Z. Zhang, L. Zhu, L. Jiang, Microbe-mediated synthesis of defect-rich CeO_2 nanoparticles with oxidase-like activity for colorimetric detection of L-penicillamine and glutathione, Nanoscale, 17 (2025) 4142-4151.

[6] W. Xu, L. Jiao, H. Yan, Y. Wu, L. Chen, W. Gu, D. Du, Y. Lin, C. Zhu, Glucose oxidase-integrated metal–organic framework hybrids as biomimetic cascade nanozymes for ultrasensitive glucose biosensing, ACS Applied Materials & Interfaces,

11 (2019) 22096-22101.

[7] X. Li, G. Lin, L. Zhou, O. Prosser, M.H. Malakooti, M. Zhang, Green synthesis of iron-doped graphene quantum dots: an efficient nanozyme for glucose sensing, Nanoscale Horizons, 9 (2024) 976-989.

[8] Z. Yuan, M. Fu, X. Wang, M. Wang, Y. Wei, Y. Sun, Q. Zhang, Y. Zhang, B. Zhang, A colorimetric strategy and smartphone-based test strip for the detection of glucose based on the peroxidase activity of a hemin-derived nanozyme, Analytical Methods, 17 (2025) 320-329.

[9] Y. Xue, Z. Chen, P. Hazelton, M. Ye, Y. Yang, C. Wang, H. Ye, S. Yang, Y. Huang, W. Zhang, X. Chen, Platinum nanoparticles/nanodiamonds nanocomposites with enhanced catalysis activity for sensitive colourimetric glucose detection, Microchemical Journal, 207 (2024) 112201.

[10] J. Xin, C. Shu, Y. Fu, X. Yu, Z. Wang, X. Zeng, R. Wang, T. Meng, J. Sun, M. Yan, MOF-confined ultrafine nanozymes with enhanced catalysis for sensitive colorimetric detection of glucose, Talanta, 283 (2025) 127152.